Low-loss Millimeter-wave Phase Shifters Based on Mechanical Reconfiguration

P. Romano[1], **O. Araromi**[2], **S. Rosset**[2],
J. Perruisseau-Carrier[3], **H. Shea**[2], **and J. R. Mosig**[1]

[1]Laboratory of Electromagnetics and Acoustics (LEMA)
École Polytechnique Fédérale de Lausanne (EPFL), Switzerland
[2]Microsystems for Space Technologies Laboratory
École Polytechnique Fédérale de Lausanne (EPFL), Switzerland
[3]Deceased. Adaptive MicroNano Wave Systems
École Polytechnique Fédérale de Lausanne (EPFL), Switzerland

Abstract— We propose different concepts of mechanically reconfigurable true-time-delay phase shifters using micro-actuators at millimeter-waves (MMW). The mechanical reconfiguration allows to achieve phase shift reconfiguration with very low losses. One of the proposed concepts has been fully implemented and tested, demonstrating state-of-the-art performance in terms of phase-shift/loss ratio.

1. INTRODUCTION

Reconfigurable phase shifters are critical components in modern communications and remote sensing systems at millimetre-wave (MMW). In general, advanced reconfiguration capabilities are increasingly required to dynamically update antenna characteristics, such as coverage, polarization or operating frequency [1, 2]. Different technologies are currently available for the implementation of tunable phase shifters, including semiconductors, RF-MEMS, Liquid Crystal and ferroelectrics [3]. However, a common feature to all these technologies is the significant increased loss, complexity and cost with regard to non-reconfigurable devices. In this context, low-loss reconfigurability, complexity and cost are driving factors in the choice of a given technology and can constitute major limitations to future development of MMW antenna devices [1].

Here we propose the analysis, design, and implementation of mechanically reconfigurable MMW phase shifters using micro-fabricated actuators. The desired phase shift tuning is obtained modifying the physical geometry of the device in order to affect the propagation constant. Such an approach allows to completely isolate the actuation part from the electromagnetic (EM) active area, thereby achieving reconfiguration with losses comparable to the device fixed counterpart. In particular, the preliminary design and performance of three different reconfigurable concepts are presented in Section 2. The design of one concept has been further optimized to be manufactured and tested, and is described in Section 3.

2. PHASE SHIFTERS BASED ON MECHANICAL RECONFIGURATION

We propose the design of reconfigurable true-time delay (TTD) phase shifters, which are key building blocks in many array antenna systems, including wideband beamsquint-free scanning arrays. The basic idea is to affect the propagation constant of a transmission line (TL) section, thereby providing TTD. Using micro-actuators, this can be done by changing the geometry of the device, in order to modify the effective permittivity of the equivalent TL. The proposed concept can potentially be implemented using different technologies for mechanical reconfiguration. For instance electrostatic (e.g., [4, 5]), magnetic (e.g., [6, 7]), piezoelectric (e.g., [8, 9]) or electroactive polymers (e.g., [10–13]) actuators could be integrated to implement the final device. Here dielectric electroactive polymer (DEAP) actuators are used to reconfigure the fabricated phase shifter presented in Section 3.

The devices presented here consist of a fixed TL, that is microstrip, coplanar waveguide (CPW) or rectangular waveguide (RWG) loaded by a movable part (dielectric or metallic), which induces a change in the TL propagation constant β. Thus, the differential phase shift between two different states A and B is given by:

$$\Delta\phi_{AB} = -\left(\beta_B - \beta_A\right) L_{PS} \tag{1}$$

where L_{PS} is the active length of the device, that is the section directly affected by reconfiguration. When quasi-TEM TLs (e.g., microstrip or CPW) are considered, the propagation constant can be written as $\beta = \omega\sqrt{\mu_0\varepsilon_0}\sqrt{\varepsilon_{r,eff}}$. Therefore, a given phase reconfiguration is achieved modifying the effective relative permittivity $\varepsilon_{r,eff}$.

However, the dynamic control of β (i.e., of the phase) via the mechanical reconfiguration of the TL geometry necessarily comes with a simultaneous variation of the TL characteristic impedance, which will affect the matching of the phase shifter. Therefore, a "minimum mismatch" design approach [13] is applied to the presented concepts. That is, the dimensions of the fixed TL and of the loading parts in the active area are optimized to maximize the phase shift to loss figure, while simultaneously minimizing the mismatch. In particular, the optimization process is based on the maximization of two figures of merit (FoMs): the maximum differential phase shift per unit length expressed by (2) and the maximum differential phase shift per unit length per mismatch given by (3) [13]:

$$\text{FoM}_1 = \frac{\phi_B - \phi_A}{L_{PS}} \tag{2}$$

$$\text{FoM}_2 = \frac{\phi_B - \phi_A}{L_{PS}\,|\Gamma_{\max}|} \tag{3}$$

Both FoMs are normalized by the length of the active section L_{PS}, which allows to compare performance of different devices independently from their length. Moreover, all simulated results presented in Table 1 in terms of propagation constant and differential phase shift are obtained normalizing scattering parameters to the "optimal" reference impedance Z_{opt} that assures the mismatch minimization [13]. All proposed phase shifter concepts (shown in Fig. 1) are optimized to operate at Ka-band (25–40 GHz), which is of increasing interest, e.g., for commercial satellite communications.

Table 1: Performance comparison for the proposed phase shifter concepts at 35 GHz.

Concept	Actuation	$\Delta\beta_{\max}$ [rad/m]	FoM_1	FoM_1
Fig. 1(a)	In-plane	560.4	32.1	581.9
Fig. 1(b)	Out-of-plane	61.9	3.5	34.3
Fig. 1(c)	In-plane	308.5	21.5	140.6

The concept of Fig. 1(a) is based on a microstrip TL (quasi-TEM) and in-plane actuation (e.g., [10, 13]). The horizontal displacement of the central strip induces a change in $\varepsilon_{r,eff}$ due to the particular shape of the bottom dielectric: when the strip is moved in the $-\Delta x$ direction, the portion of dielectric below increases ($\varepsilon_{r,eff}$ increases), while it reduces with a displacement in the $+\Delta x$ (the air portion below the strip increases, decreasing $\varepsilon_{r,eff}$). It is clear that this effect is magnified increasing the substrate permittivity ($\varepsilon_r = 10$ is chosen for our design). The "trapezoidal" cut of the dielectric is introduced to improve the matching (impedance tapering) between the feeding (fixed) microstrip and the movable section. The compliant connections shown in Fig. 1(a) can be realized using flexible metallizations (e.g., [14]) or alternatively replaced by a capacitive coupling between fixed and movable strips. Preliminary performance reported in Table 1 assume a total displacement of 400 µm ($\Delta x = \pm 200$ µm), which corresponds to only 0.04λ at the design central frequency $f_0 = 30$ GHz. Simulated scattering parameters are shown in Fig. 2(a). Insertion loss is always lower than 1.5 dB and return loss better than 10 dB, with a phase shift/loss ratio of around 350 deg/dB at 35 GHz.

The basic idea characterizing the concept depicted in Fig. 1(b) is the variable loading of a WR-28 RWG. A metallic rod is vertically moved inside the active area by one or more out-of-plane actuators (e.g., [9, 11]), modifying the capacitance per unit length (and thus the propagation constant) of the equivalent TL. More specifically, the propagation constant increases if the metallic load is "pushed" inside the RWG (Δh increases). The loading part is properly shaped to improve the matching between the fixed and reconfigurable sections. This device has the advantage to be a "closed" structure, which is very appealing for high power applications and could be easily manufactured using standard micromachining techniques. Moreover, it does not comprise any dielectric in the EM active area. Simulated performance of Table 1 refer to a total vertical displacement $\Delta h = 1$ mm. Simulated results of Fig. 2(b) predict an insertion loss lower than 0.6 dB and a return loss better than 15 dB. The mean phase shift/loss ratio is around 180 deg/dB at 35 GHz.

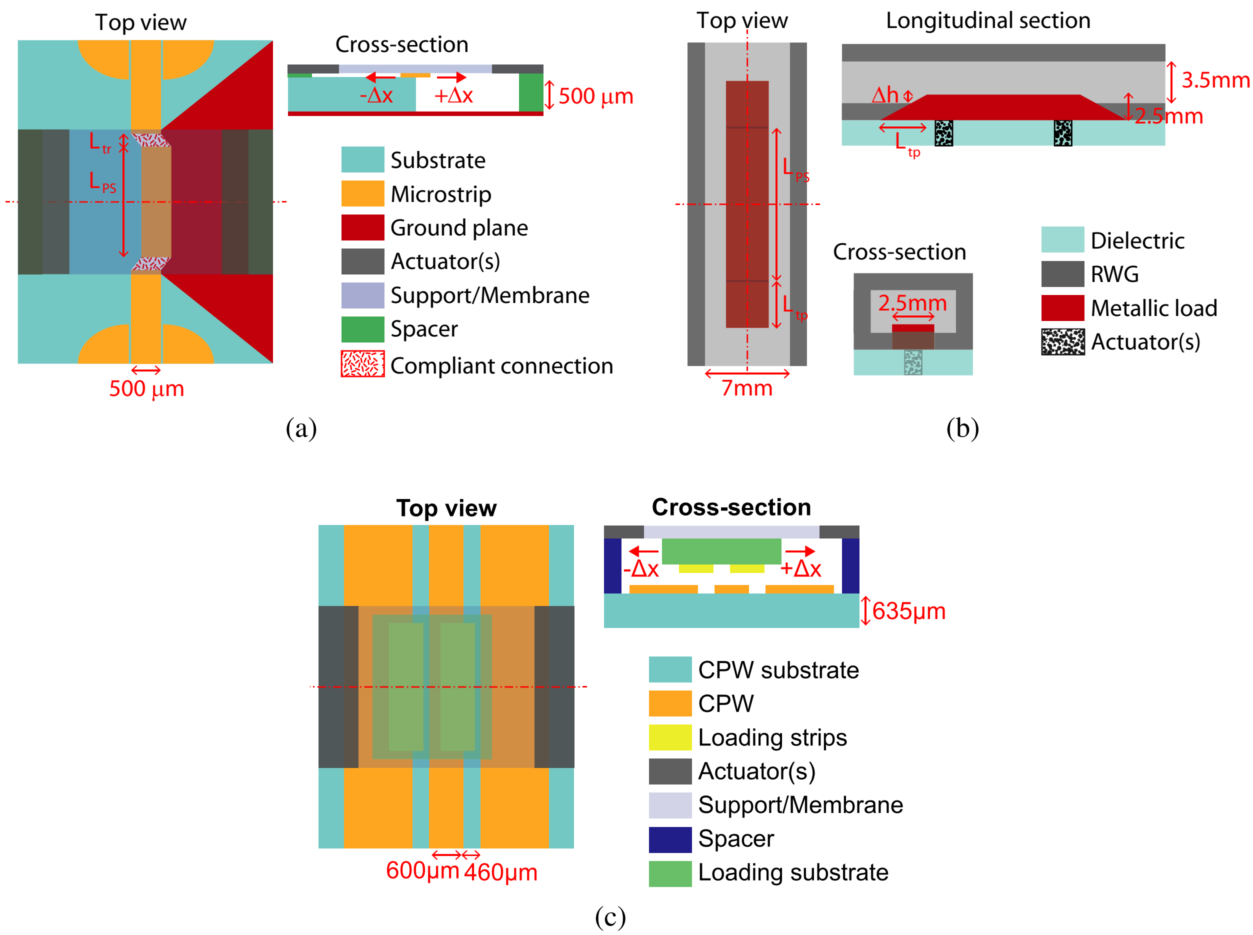

Figure 1: Simplified drawing of the proposed phase shifter concepts. (a) Reconfigurable phase shifter based on a microstrip TL: the central section can be reconfigured modifying the effective relative permittivity. (b) Rectangular waveguide loaded by a metallic rod that can be displaced in the vertical direction affecting the capacitance per unit length of the equivalent TL. (c) Reconfigurable concept based on a conventional CPW loaded by two suspended metallic strips, which are horizontally displaced by in-plane actuators.

The phase shifter concept illustrated in Fig. 1(c) consists of a conventional coplanar waveguide (CPW) loaded by two suspended metallic strips (their spacing is constant), which are supported and horizontally displaced in the $\pm\Delta x$ direction by in-plane actuators. The actuation part also assures that the vertical spacing between the CPW and the strips keeps constant. Simulated performance of Table 1 assume a total horizontal displacement of 530 µm ($\Delta x = \pm 265$ µm) [13].

The results presented in Table 1 and Fig. 2 highlight very good performance for the microstrip-based concept of Fig. 1(a) that exhibits a phase shift per unit length of 32.1°/mm with very low losses. The RWG concept (Fig. 1(b)) presents lower phase shift performance with extremely low losses (only ohmic), but can be suitable for high power applications. However, the achievable phase shift can be increased replacing the metallic load with a high permittivity dielectric (adding dielectric losses). The device of Fig. 1(c) exhibits the best trade-off between performance and low-cost/low-complexity fabrication process. In fact, it does not require any flexible/compliant connection between the movable and fixed part (in contrast with the concept shown in Fig. 1(a)), and can be easily prototyped (and tested) using standard manufacturing techniques and in-house available technology. Thus, it was selected to be fabricated and tested. A detailed description of the manufacturing and test of the proposed reconfigurable phase shifter is given in Section 3.

3. IMPLEMENTATION AND MEASUREMENTS

3.1. Reconfiguration Approach

Dielectric electroactive polymer (DEAP) actuators are selected to implement the proposed phase shifter reconfiguration (Fig. 1(c)) [13]. DEAPs, also known as artificial muscles, consist of an elas-

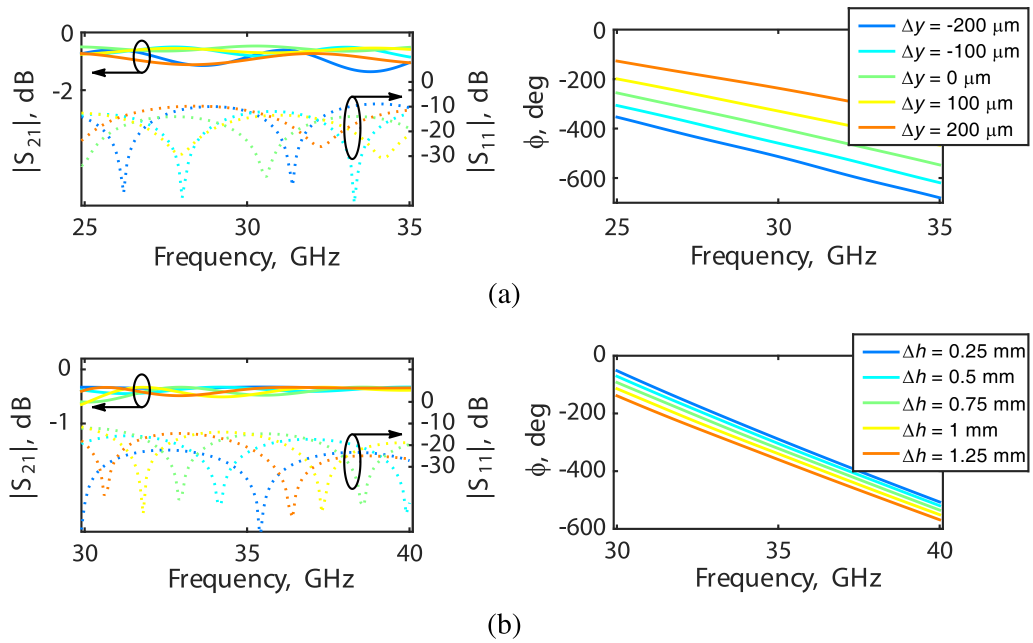

Figure 2: Simulated scattering parameters for different states of reconfiguration. (a) Concept of Fig. 1(a): $L_{PS} = 10\,\text{mm}$, $L_{tr} = 200\,\mu\text{m}$, substrate with $\varepsilon_r = 9.8$ and $\tan\delta = 0.002$ (e.g., Rogers TMM10i). The compliant connections are modeled as a resistive sheet with $R_S = 30\,\Omega/\square$ [14]. (b) Concept of Fig. 1(b): $L_{PS} = 20\,\text{mm}$, $L_{tp} = 5\,\text{mm}$. A conductivity $\sigma = 2.9 \times 10^7\,\text{S/m}$ is considered for all metallic parts, and actuators are completely shielded from the EM active area.

tomer membrane sandwiched between two compliant electrodes. The subsequent application of a voltage bias across the electrodes results in thickness compression and large (over 200%, [10]) in-plane area expansion. In addition, DEAPs provides mechanical actuation with low cost materials and fabrication, low device complexity, large strain, reduced size and bulkiness and analogue operation. DEAPs currently typically require high actuation voltage (in the kilovolt range) to achieve large strain expansion. This high voltage is considered an acceptable drawback given the advantages brought by the DEAP technology. The required voltages can be readily obtained using commercial DC-DC converters fitting in less than $2\,\text{cm}^2$. Moreover, it is worth noting that currents are very small and power is only required to change the device configuration (and not to hold a constant position), hence providing very low power actuation.

A detailed drawing of the phase shifter cross section is shown in Fig. 3(a). The needed horizontal displacement of the loading strips is realized by two antagonist planar DEAP actuators, which are integrated in the polydimethylsiloxane (PDMS) membrane. They are composed of carbon black

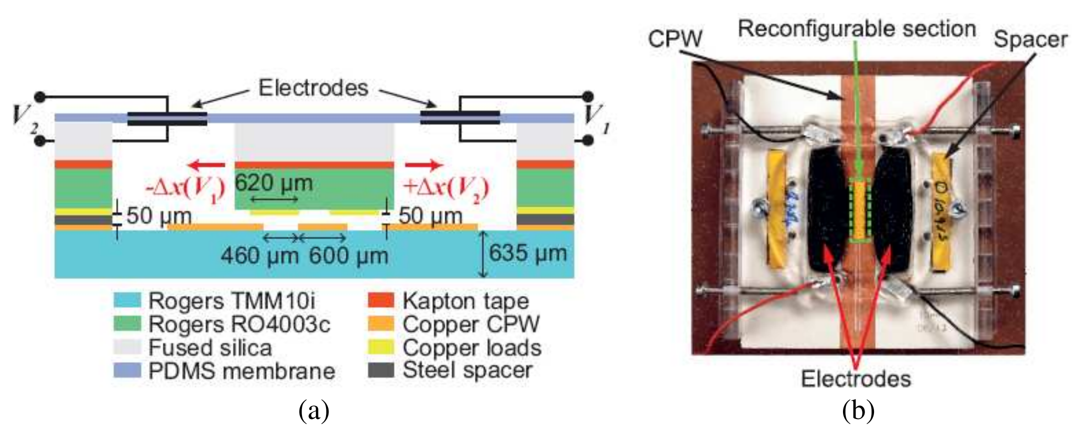

Figure 3: Manufactured reconfigurable phase shifter. (a) Simplified cross-section drawing of the proposed phase shifter concept. (b) Picture (top view) of the fabricated prototype.

particles in a PDMS matrix and are applied using a stamping method. As a result of the actuation, the loading part, fixed to a passive region in the center of the membrane, is displaced linearly in-plane. In particular, a voltage V_1 induces a movement $-\Delta x$ (towards minimum phase shift), while a voltage V_2 generates a movement of $+\Delta x$ (towards maximum phase shift) in the opposite direction (Fig. 3). Such an approach allows to completely isolate the actuator part from the EM active area (Fig. 3), providing phase shift reconfiguration with very low losses (only ohmic and dielectric losses), as it is demonstrated by the experimental characterization of the manufactured prototype presented in 3.2.

3.2. Design, Fabrication and Test

The design process is optimized to comply with all the constraints imposed by the EAP technology and the manufacturing techniques available in our laboratory. The device assembly (cross-section) with the materials used and relevant dimensions of the reconfigurable section are shown in Fig. 3(a). The length of the reconfigurable section is fixed to 10 mm for the presented prototype, but can be subsequently selected according to the phase shift requirement for a given application, since these two quantities are directly proportional (TTD phase shifter).

The final prototype is designed to be modular and manually assembled; this allows us to use the same CPW TL with different reconfigurable parts (for testing purposes) and to replace single pieces in case of local failure. Therefore, the different components are fabricated separately using commercial materials (Fig. 3(a)) and standard printed circuit board (PCB) fabrication processes (avoiding cleanroom activities), thus reducing manufacturing complexity and obtaining a very low-cost prototype. The fabricated phase shifter based on DEAP reconfiguration is shown in Fig. 3(b).

Probe-based 2-port scattering parameters measurements are used to characterize the fabricated prototype of Fig. 3(b) in the range 25–35 GHz. A thru-reflect-line (TRL) calibration is used to remove the effect of the transitions between the coaxial-based network analyzer and the CPW-based device and to place the measurement reference planes at the edges of the reconfigurable section. Measured scattering parameters in the full frequency range are reported in Fig. 4. The fabricated phase shifter provides a maximum analog phase range (i.e., between maximum and minimum displacement) of around 180° at 30 GHz with extremely low losses. The insertion loss is in fact always lower than 1.6 dB with an average value of 0.83 dB over the total frequency range. The return loss is always better than 11 dB, which means good matching for all the phase shifting states in the whole 10 GHz bandwidth. The low-loss phase shift reconfiguration demonstrated by experimental results, allows state-of-the-art performance in terms of the most important figure of merit for TTD phase shifters, namely, the phase-shift/loss ratio. Indeed, a mean value of 235°/dB is achieved at 35 GHz, considerably outperforming semiconductor phase shifters at similar frequencies (e.g., [15]). Moreover, it also compares well to lower-loss state-of-the art MEMS reconfigurable phase shifters (e.g., [16]). In addition, the device proposed here offers a large analog tuning range, which represents an advantage over the digital behavior of its MEMS and MMIC counterparts. It is worth noting that the total phase range can be increased using longer loading lines (TTD principle, Eq. (1)).

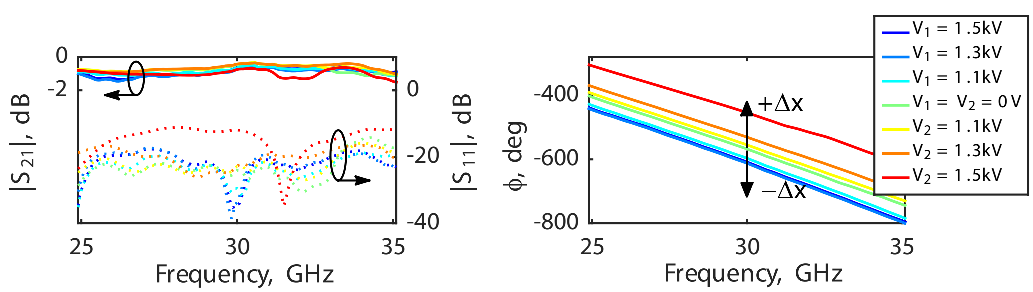

Figure 4: Measured scattering parameters in the range 25–35 GHz for the fabricated phase shifter of Fig. 3(b). Different reconfiguration states are shown, i.e., $V_1 = V_2 = 0$ kV, $V_1 = 1.1$, 1.3, 1.5 kV, $V_2 = 1.1$, 1.3, 1.5 kV.

4. CONCLUSION

The phase shift performance of three different mechanically reconfigurable concepts operating at Ka-band have been presented. All the proposed phase shifters are based on a fixed TL perturbed by loading elements, which are displaced using micro-actuators. The optimized design, fabrication and experimental characterization of a CPW-based concept have been reported, highlighting excellent phase shift to loss figure of merit (235°/dB at 35 GHz).

ACKNOWLEDGMENT

This work was supported by the European Space Agency (NPI project REACT) and the Swiss National Science Foundation (SNSF) under Grant No. 133583. The authors would like to thank Jean-Christophe Angevain (Antenna and Sub-Millimeter Wave Section, ESA ESTEC) for stimulating discussion.

REFERENCES

1. Mangenot, C. and G. Toso, "European space technology harmonisation technical dossier on array antennas european space agency," *ESTEC, TEC-EEA*, Noordwijk, 2012.
2. Arrebola, M., J. A. Encinar, R. Cahill, and G. Toso, "Dual-reflector antenna with a reflectarray subreflector for wide beam scanning range at 120 GHz," *2012 Int. Conf. Electromagn. Adv. Appl.*, 848–851, 2012.
3. Hum, S. V. and J. Perruisseau-Carrier, "Reconfigurable reflectarrays and array lenses for dynamic antenna beam control: A review," *IEEE Trans. on Antennas Propag.*, Vol. 62, No. 1, 183–198, 2014.
4. Legtenberg, R., A. W. Groeneveld, and M. Elwenspoek, "COMB-drive actuators for large displacements," *J. Micromech. Microeng.*, Vol. 6, 320–329, 1996.
5. Chen, C., C. Lee, Y.-J. Lai, and W. Chen, "Development and application of lateral COMB-drive actuator," *Jpn. J. Appl. Phys.*, Vol. 42, 4059–4062, 2003.
6. Cugat, O., J. Delamare, and G. Reyne, "Magnetic micro-actuators and systems (MAGMAS)," *IEEE Trans. Magn.*, Vol. 39, No. 6, 3607–3612, 2003.
7. Hage-Ali, S., Y. Orlic, N. Tiercelin, R. Sauleau, P. Pernod, V. Preobrazhensky, and P. Coquet, "A millimeter-wave elastomeric microstrip phase shifter," *2012 IEEE MTT-S*, Jun. 17–22, 2012.
8. Kim, S.-G., T.-Y. Yun, and K. Chang, "Time-delay phase shifter controlled by piezoelectric transducer on coplanar waveguide," *IEEE Microw. Wireless Compon. Lett.*, Vol. 13, No. 1, 19–20, Jan. 2003.
9. Wu, J., J. Lou, M. Li, G. Yang, X. Yang, J. Adams, and N. X. Sun, "Compact, low-loss, wide-band, and high-power handling phase shifters with piezoelectric transducer-controlled metallic perturber," *IEEE Trans. Microw. Theory Techn.*, Vol. 60, No. 6, 1587–1594, 2012.
10. Pelrine, R., R. Kornbluh, Q. Pei, and J. Joseph, "High-speed electrically actuated elastomers with strain greater than 100%," *Science*, Vol. 287, No. 5454, 836–839, 2000.
11. Carpi, F., G. Frediani, and D. De Rossi, "Hydrostatically coupled dielectric elastomer actuators," *IEEE-ASME Trans. Mecchatron.*, Vol. 15, No. 2, 308–315, 2010.
12. Shea, H., "Miniaturized EAPs with compliant electrodes fabricated by ion implantation," *Electroactive Polymer Actuators and Devices (EAPAD) 2011*, Vol. 7976, May 2011.
13. Romano, P., O. Araromi, O., S. Rosset, H. Shea, and J. Perruisseau-Carrier, "Tunable millimeter-wave phase shifter based on dielectric elastomer actuation," *Appl. Phys. Lett.*, Vol. 104, No. 5, 024104, 2014.
14. Romano, P., S. Rosset, L. Maffli, H. Shea, and J. Perruisseau-Carrier, "Electromagnetic characterisation of flexible conductive membranes at millimetre-waves," *Electron. Lett.*, Vol. 49, No. 5, 353–354, 2013.
15. Yang, J. G. and K. Yang, "Ka-band 5-bit MMIC phase shifter using InGaAs PIN switching diodes," *IEEE Microw. Wireless Compon. Lett.*, Vol. 21, No. 3, 151–153, 2011.
16. Hayden, J. S. and G. M. Rebeiz, "Very low-loss distributed X-band and Ka-band MEMS phase shifters using metal-air-metal capacitors," *IEEE Trans. Microw. Theory Techn.*, Vol. 51, No. 1, 309–314, 2003.